Theoretical Study of the Kinetics of the Hydrogen Abstraction from Methanol. 1. Reaction of Methanol with Fluorine Atoms

Jerzy T. Jodkowski,[†] **Marie-Thérèse Rayez,*** and **Jean-Claude Rayez**

Laboratoire de Physicochimie Moléculaire, CNRS UMR 5803, Université Bordeaux 1, 351, Cours de la Libération, 33405 Talence, France

Tibor Bérces and Sándor Dóbé

Central Research Institute for Chemistry, Hungarian Academy of Sciences H-1525 Budapest, Hungary

Ab initio calculations at different levels of theory and using several basis sets were performed for the title two-channel hydrogen-abstraction reaction. Conclusions are drawn from G2 energies. These calculations have shown that this reaction, which can give two products (namely, CH_3O and CH_2OH), proceeds through the formation of intermediate complexes followed by transition states with quite negligible activation energy. We propose a method for the calculation of the rate constant of a bimolecular reaction proceeding through the formation of two intermediate complexes. General equations, taking into account the rotational energy, are derived from RRKM theory, using the simplified version of the SACM theory. The resulting calculated overall rate constant as well as the yield of the methoxy branching ratio are in very good agreement with experimental findings. The expressions for the site-specific rate constants $k(CH_3O)$ and $k(CH_2OH)$ allow the description of the reaction kinetics over a wide range of temperatures. A temperature rate constant fit, convenient for chemical modeling studies, is $k(CH_3O) = 1.0 \times 10^{-10} (T/300)^{0.5}$ cm^3 molecule^{-1} s^{-1} and $k(CH_2OH) = 6.9 \times 10^{-11} (T/300)^{0.27}$ cm^3 molecule^{-1} s^{-1}.

1. Introduction

The fact that methanol is considered one of the most attractive alternative fuels has been confirmed in several economic and practical combustion studies.[1,2] Its combustion leads to genera- tion of less air pollutants compared to gasoline. Moreover, it has a higher octane number, a leaner flammability limit, and a higher flame speed. The hydrogen abstraction reaction from methanol is then of primary importance from both experimental and theoretical points of view. Reaction of H-abstraction by fluorine atoms is known as an efficient method for the production of either free radicals or rovibrationally excited HF molecules.[3] Due to the presence of nonequivalent hydrogen atoms in methyl and hydroxyl groups, the H-abstraction from methanol by fluorine atoms leads to the formation of both methoxy and hydroxymethyl radicals according to the following competitive reaction channels

$$CH_3OH + F \rightarrow CH_3O + HF \qquad (R1)$$

$$\rightarrow CH_2OH + HF \qquad (R2)$$
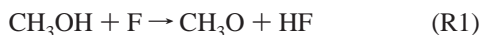
The highly reactive primary radical products formed in the parallel reaction channels may initiate different subsequent reactions as well as interference with each other. Therefore, knowledge of the values of the branching ratios which describe the relative efficiencies of reaction channels is of fundamental importance for the combustion and atmospheric modeling studies.

The $CH_3OH + F$ reaction system was an object of quite intensive experimental investigations in the past decade using either indirect[4] or direct[5] methods. However, the reported values of the branching ratios are very different from one study to the other, showing serious experimental uncertainties. However, nearly all the experimental results indicate an anomalously efficient methoxy yield for the methoxy branching fraction (R1) greater then 50%. In particular, the measurements of Durant[5e] lead to a value of the methoxy branching ratio of 0.6 ± 0.2 at room temperature, and to temperature independent branching ratios for the mixed isotopomers (CH_3OH and CH_3OD).

This is contrary to the expectation based on thermochemical and statistical considerations. Both reaction channels are highly exothermic, with reaction enthalpy of -39.9 and -30.8 kcal/ mol for the hydroxymethyl (R2) and methoxy (R1) channels, respectively. A greater exothermicity of R2, and the presence of three equivalent hydrogen atoms of the methyl group is in favor of the formation of hydroxymethyl radicals (R2). Domi- nance of this reaction channel is experimentally observed for the H-abstraction from methanol by chlorine,[5f] bromine,[5f] hydrogen atoms, and hydroxyl and methyl radicals.[6] In a very recent investigation of Dóbé et al.,[5f] the branching ratios for both CH_2OH and CH_3O radical formation were determined for the first time in the same study and under comparable experimental conditions. The value obtained for the methoxy branching fraction of 0.57 ± 0.05 seems to be the most credible one. Anomalous high methoxy yields for H-abstraction from methanol by fluorine atoms suggest the possibility of other reaction mechanisms for this reaction. Very high value of the overall rate constant (R1 + R2) indicates small or negligible energy barriers for both reaction channels. Therefore, one can

---

[†] Permanent address: Department of Physical Chemistry, Wroclaw University of Medicine, Pl. Nankiera 1, 50-140 Wroclaw, Poland.
* To whom correspondence should be addressed.

expect that the branching ratio values are determined by the differences in activation entropies rather than in activation energies for the R1 and R2 channels.

Only one theoretical study related to the $CH_3OH + F$ reaction system is reported in the literature (Glauser and Koszykowski[7]). They applied ab initio calculations of intermediate complexity in conjunction with conventional transition state theory to obtain transition state structures and rate constants for both reaction channels. Results of their calculation allow a semi quantitative description of the kinetics of the reaction under investigation. Derived values of the branching ratios are in satisfactory agreement with experiment. However, uncertainties in the knowledge of some parts of the potential energy surface diminish the reliability of the final results. A transition state for hydroxyl-side fluorine attack (leading to methoxy radical formation) has not been found by Glauser and Koszykowski. Therefore, the structure of the hydrogen-bonding molecular complex, $CH_3OH\cdots F$, and its vibrational levels (with conversion of the lowest vibrational mode to imaginary frequency) were adapted in their calculation to model the 'transition state' for hydroxyl-side attack. That approach, which implies a zero-energy barrier for the methoxy formation, favors this channel. Moreover, the value of the overall rate constant obtained theoretically still remains about five times lower than the one observed experimentally. Glauser and Koszykowski have also found an additional saddle point for HF-catalyzed isomerization of the methoxy and hydroxymethyl products. The total energy of this transition state was very close to the reactants energy. However its role and the dynamical implications for the $CH_3OH + F$ reaction system were not explained and discussed despite of some similarity with the hydrogen-bonding complex, $CH_3OH\cdots F$, which may argue in favor of the methoxy reaction channel.

The primary aim of the present investigation is to find an explanation of anomalous experimental findings and to obtain a better understanding of the kinetics of H-abstractions in the $CH_3OH + F$ reaction system. Therefore, we carried out calculations using molecular orbital theory in order to locate and characterize the relevant stationary points (reactants, products, intermediate complexes, and transition states) on the potential energy surface. Results of these calculations provide the starting point for computational methods of the reaction rate theory (described in section 3) which will enable us to evaluate the site-specific reaction rate constants and the branching ratios over a wide range of temperatures.

2. Electronic Structure Calculations

2.1. Computational Details. The ab initio MO calculations were carried out using GAUSSIAN 92 and GAUSSIAN 94 programs.[8] Restricted Hartree–Fock (RHF) self-consistent field (SCF) wave functions were used for closed-shell molecules (CH_3OH and HF), whereas unrestricted Hartree–Fock (UHF) SCF wave functions were used for the other open-shell species.[9] Electron correlation energy was calculated using Møller–Plesset many body perturbation theory[10] with RHF or UHF wave functions as a reference. The geometries of all minimum energy structures and saddle points (reactants, products, intermediate complexes, and transition states) were fully optimized using analytical gradients at SCF and MP2 levels with both 6-31G* and 6-311G** basis sets. The single-point energy calculation at MP4 level including single, double, triple and quadruple excitations (MP4SDTQ) were also performed in "frozen core" approximation for all stationary points based on geometries optimized at the MP2/6-311G** level.[8] Total energies for open-

shell species (denoted as PMPn) were calculated using a projection method included in the Gaussian program. Total energies were also determined at G1 and G2 levels of theory.[11] This last approach, which requires some additional calculations of types MP4/6-311G**, MP4/6-311+G**, MP4/6-311G(2df,p), MP2/6-311+G(3df,2p), and QCISD(T)/6-311G** using the MP2/6-31G* optimized geometry as reference, leads to a significant improvement of the calculated total energy. Temperature corrections to the total energies and ideal-gas thermodynamic functions were calculated (assuming no free and internal rotations) in the classical rigid-rotor and harmonic-oscillator approximation using the vibrational frequencies obtained in the (U)HF/6-31G* calculation scaled by the factor of 0.8929. For open-shell molecular systems the UHF SCF wave functions are not eigenfunctions of $\langle S^2 \rangle$, and can be contaminated by higher multiplet states. It was found that spin contamination increases calculated energy barriers.[12] However, in the present calculations expectation values of $\langle S^2 \rangle$ for all UHF wave functions did not exceed 0.78 so that effects of spin contamination can be neglected.

2.2. Results for the geometries and Vibrational Frequencies. At all levels of theory, the search for each stationary point was made independently. Optimized geometries and vibrational frequencies calculated at the MP2/6-311G** are collected in Tables 1a and b. These properties, obtained at the MP2/6-31G* are given as supplementary material in Tables IaS and IbS (see Supporting Information).

Methanol. The equilibrium geometry of methanol corresponds to a staggered conformation of C_s symmetry. There are two sites for the hydrogen abstraction from methanol by fluorine atom: one for the hydroxyl-side attack and another for the methyl-side attack of fluorine.

Molecular Complex $CH_3OH\cdots F$ (MC1a). At all levels of theory, the geometrical parameters of this hydrogen-bonding complex, $CH_3OH..F$, denoted by MC1a (Figure 1) are conserved as in isolated methanol. The $H_o\cdots F$ optimized distance varies from 2.22 Å with the 6-31G* basis set to 2.35 Å for the 6-311G** basis set, showing that the presence of polarization functions leads to looser complexes. The thermal stability of MC1a with respect to the reactants energy is estimated to be 0.7–1.6 kcal/mol at 0 K depending on the level of theory used.

Transition State $CH_3O\cdots H\cdots F$ (TS1). The transition state corresponding to abstraction of the hydrogen atom from hydroxyl group of methanol is shown in Figure 1 and Table 1 and is denoted as TS1. The structure of this saddle point is roughly the same whatever the basis set. At SCF level, TS1 retains the C_s symmetry of methanol, whereas at MP2 level, the $F-H_o-O-C$ skeleton is about 23° out of the H_o-O-C plane. The breaking bond distance $O-H_o$ and the forming $F\cdots Ho$ bond are respectively equal to 1.01 and 1.35 Å at MP2/6-311G**. These values are consistent with the corresponding ones, 1.03 and 1.29 Å, for the transition state obtained at MP2/6-31G** level for the analogous hydrogen abstraction reaction $H_2O + F \rightarrow HF + OH$.[14] The angle OH_oF is the most sensitive structural parameter, as it varies from 157° in UHF/6-31G* to 118° in MP2/6-31G* calculation. The normal mode having the imaginary frequency is the $O\cdots H_o\cdots F$ asymmetric stretching and corresponds to the direction of the reaction coordinate.

Molecular Complex $CH_3O\cdots HF$ (MC1b). At any level of theory, the molecular complex of methoxy radical with hydrogen fluoride $CH_3O\cdots HF$ (MC1b) is the most stable structure for the methoxy reaction channel. The $O\cdots H_o$ distance, 1.79 Å (MP2/6-311G**) is ca. two times longer than the OH bond in methanol. The $H_o\cdots F$ bond length is close to that in HF

Hydrogen Abstraction from Methanol. 1

J. Phys. Chem. A, Vol. 102, No. 46, 1998 **9221**

TABLE 1: Optimized Structures and Vibrational Frequencies of Stationary Points of the Potential Energy Surface Obtained at the MP2/6-311G** Level

	MC1a	TS1	MC1b	TS2	MC2	MC3	TS3
				(a) Optimized Structures			
CO	1.4168	1.4260	1.3837	1.3975	1.3775	1.4206	1.2892
OH_o	0.9575	1.0063	1.7858	0.9593	0.9599	0.9588	1.2877
CH_a	1.0904	1.0911	1.0926	1.0905	1.0794	1.0897	1.0911
CH_b	1.0973	1.0912	1.1015	1.1343	2.5415	1.0959	1.3263
CH_c	1.0973	1.0925	1.0952	1.0951	1.0833	1.0963	1.1084
H_oF	2.3478	1.3528	0.9258				
H_bF				1.5141	0.9240		1.3830
FO						2.3907	
COH_o	106.0906	108.3526	100.5047	106.7084	108.7549	106.6261	95.4677
OCH_a	106.9738	105.6687	112.5934	108.1347	112.2759	106.7038	119.0894
OCH_b	112.4464	110.8724	105.1450	111.6727	40.8772	112.1492	91.0564
OCH_c	112.4464	111.6755	110.7869	113.9527	117.2884	112.0111	119.0423
OH_oF	152.1706	120.6946	157.0194				
CH_bF				142.8758	134.8629		126.8248
COF						102.8566	
H_oOCH_a	180.0000	−156.8433	−167.1425	178.6930	−178.4532	178.1987	−145.2058
H_oOCH_b	61.4057	84.8595	73.8655	62.5283	−38.0320	59.7479	−19.7729
H_oOCH_c	−61.4057	−37.8624	−40.4958	−58.1829	34.9006	−63.2738	64.9716
FH_oOC	0.0000	−77.5349	−3.5161				
FH_bCO				−59.5778	−176.3830		28.2964
$FOCH_a$						77.6438	
				(b) Vibrational Frequencies			
v_1	60	140	90	55	73	72	377
v_2	66	214	126	174	128	84	547
v_3	103	294	237	388	233	121	663
v_4	363	1042	542	1002	457	367	684
v_5	1093	1088	743	1118	629	1085	1103
v_6	1118	1194	919	1163	742	1108	1200
v_7	1199	1299	1068	1325	761	1197	1267
v_8	1412	1492	1180	1431	1094	1398	1296
v_9	1516	1502	1411	1459	1205	1515	1521
v_{10}	1518	1531	1460	1517	1385	1518	1585
v_{11}	1537	2591	1541	2197	1519	1535	1740
v_{12}	3044	3085	3026	3094	3193	3055	2033
v_{13}	3107	3184	3114	3192	3348	3125	2963
v_{14}	3182	3195	3171	3913	3915	3192	3176
v_{15}	3943	2128i	3962	747i	4005	3917	2465i

[a] Bond lengths in Å, valence and dihedral angles in degrees.

molecule. The vibrational frequency of O-H_o stretch increases significantly at the SCF level and only slightly at the MP2 level compared to the corresponding mode in isolated methanol. Thermal stability of MC1b depends on the level of theory. In G2 calculations the total energy of Mclb at 0 K is about 5.2 kcal/mol lower than the methoxy channel products.

Transition State F···H···CH2OH (TS2). The transition state TS2 corresponds to the abstraction of the hydrogen from the methyl group of methanol as shown in Figure 1. Glauser and Koszykowski found to different transition state structures TS2s (corresponding to H-abstraction from position *syn* of methyl relative to OH group) and TS2a (related to the position *anti*). In fact, TS2a is not a true transition state, as its small imaginary frequency (about 100i cm^{-1}) corresponds to an internal rotation of the methyl group which disappears when the C_s symmetry constraint is removed in the saddle point searching procedure. The true transition state is located for H_a lying 60°out of the C−O−H_o plane. Therefore abstraction of any hydrogen atom of methyl group of methanol is related to the same transition state TS2. Either SCF or MP2 calculations show that the attack of the fluorine atom is far from collinear at the transition state. The relative increase of the O−H breaking bond length at the transition state with respect to its equilibrium value in methanol is about 0.05 Å in MP2. The increase of the H···F forming bond length is of the order of 0.57 Å (MP2). This corresponds to an early transition state, which is consistent with the high exothermicity of this channel.

Molecular Complex FH···CH2OH (MC2). The molecular complex hydroxymethyl (Table 1, Figure 1) with hydrogen fluorine, MC2, is the most stable structure in the CH3OH + F overall reaction system. In this structure, there is a long distance interaction between CH2OH and the molecule HF. The characteristics of CH2OH and HF (H_b−F only 5% longer than in isolated HF) are almost conserved. The F−H_b···O structure is nearly collinear. The contact O···H_b distance of 1.75 Å in MC2 is close to the value of 1.79 Å obtained for MC1b at the MP2/6-311G** level. Total energies (including ZPE) are below the hydroxymethyl channel products by 6.4 kcal/mol at MP2/6-311G** and MP4/6-311G**//MP2/6-311G** levels and by 4.9 kcal/mol at the G2 level.

Molecular Complex (MC3). MC3 is a loose molecular complex. The distances between the attacking fluorine atom and the atoms of the methanol are long; the shortest one corresponds to F···O equal to 2.4 Å, while the F···H distances are longer: 2.7 and 2.9 Å for hydrogen of hydroxyl and methyl group, respectively, at the MP2/6-311G** level. The MC3 structure is similar at all levels of theory. The total energy of MC3 predicts its thermal stability towards reactants to be 2.0− 3.6 kcal/mol depending on the method used (the most realistic seems to be the G2 value of 3.5 kcal/mol at 0 K).

Cyclic Transition State (TS3). The optimized structure of the cyclic transition state displayed in Table 1 and shown in Figure 1 strongly depends both on the method and basis set used, and is in basic agreement with structures found by Glauser
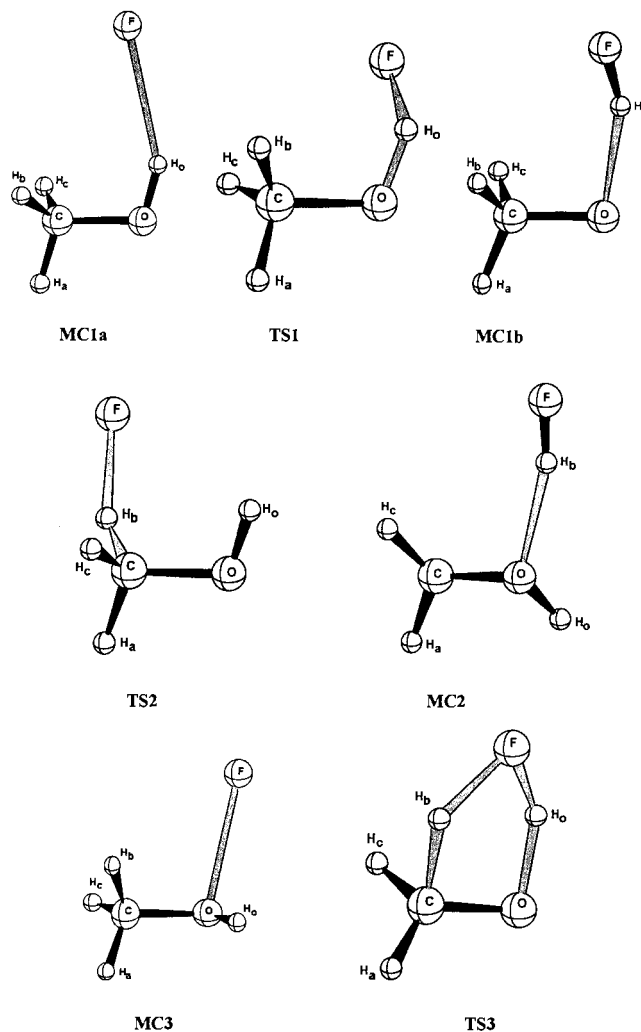
Figure 1. Configurations of the intermediate structures.

and Koszykowski at the MP2 level with the 6-31G** basis set. Indeed TS3 is a transition state for the HF catalyzed isomerization of CH_2OH to CH_3O, and may play an important role in the reaction mechanism as it can be involved in both reaction channels.

2.3. Energetics and Mechanism. In Tables IIS and IIIS of the Supporting Information are given details of the total energy calculations at the different levels of theory and basis sets used for all the characteristic points of the potential energy surface of the $CH_3OH + F$ reaction system. In Table 2 are shown the relative energies (including zero-point vibrational energy corrections, ZPE) of the stationary points at different levels of theory with respect to the reactants energy. This table also includes the calculated reaction enthalpy values at 298 K. The use of the G2 methodology (or its less sophisticated versions: G2MP2, G2MP3, or G1)[11] leads to a significant improvement in the heat of reaction values, especially for the methoxy reaction channel. The small differences for reaction enthalpies obtained using G1, G2, G2MP2, and G2MP3 calculations lead to the conclusion that the G2MP2 method is the most economic way of energy improvement.

The mechanism of the hydrogen abstraction from methanol by fluorine atoms is quite complex. This apparently elementary gas-phase reaction proceeds through the formation of intermediate complexes. The energy profiles obtained at the G2 level are shown in Figure 2. Figures 2a and b show the energy diagram with and without zero-point vibrational energy cor-

rection, respectively. Attack of the fluorine atom on the hydroxyl group of methanol leads at first to the formation of the hydrogen-bonded molecular complex MC1a, then, in a second step, via transition state TS1, it forms the methoxy−HF molecular complex MC1b, which dissociates into the methoxy channel products. The reaction pathway concerning the fluorine atom attack on the methyl group of the methanol molecule, also consists of three elementary steps. In the first step, the molecular complex MC3 is formed, and then, via the corresponding transition state $F\cdots H\cdots CH_2OH$ (TS2), leads to the molecular complex hydroxymethyl−HF, MC2, which yields the hydroxymethyl channel products. There is a third possible reaction pathway which, from MC3, proceeds, through the cyclic transition state, TS3, to the methoxy channel products. The transition state TS3 may play an important role in the reaction mechanism by increasing the yield of the CH_3O production. Some methoxy radicals are then also formed by a methyl-side attack of the fluorine atom. In particular, this may explain the value of the methoxy branching ratio observed experimentally for the reaction of methanol with fluorine, which is considerably higher than expected, in comparison with analogous reactions such as CH_3OH with Cl, Br, H, and OH.

Adding the zero-point vibrational energy leads to a situation in which transition states previously found have total energies lower than molecular complexes and reactants. This is illustrated by Figure 2b. At the G2 level, TS2 and TS3 are respectively located 3.2 and 1.2 kcal/mol below the MC3 energy. Also TS1 is energetically located 1.8 kcal/mol below MC1a. One can expect that the main sources of possible G2 uncertainties are related to the so-called higher level correction (HLC) and the ZPE estimation. The HLC corrects empirically for missing correlation energy for spin-paired electrons. This term, which depends only on the number of valence α- and β-electrons, may be less appropriate for transition states than for bound structures. Moreover, the differences in the calculated structural parameters of transition states obtained at the different levels of theory are considerably greater than for the stable structures. This is especially obvious for TS1 and TS3. However, results of calculations obtained at the more sophisticated MP2/6-311G** level also lead to the total energy of TS3 1.5 kcal/mol lower than MC3, and 3.5 kcal/mol below the energy of the reactants.

In the G2 approach, the zero-point vibrational energy is calculated using (U)HF/6-31G* frequencies scaled by the factor 0.8929 (1/1.12). While this leads to a realistic estimation of the ZPE for stable molecules, it can be different for the transition states. A good estimation of ZPE can be also obtained using MP2-frequencies scaled typically by 0.94. The most significant differences in SCF (scaled by 0.8929) and MP2 (scaled by 0.94) values of ZPE are those related to the transition states: TS1 of 26.9 and 29.3 kcal/mol, and TS2 of 27.7 and 29.6 kcal/mol calculated from scaled SCF/6-31G* and MP2/6-311G** frequencies, respectively. For the other molecular structures the differences do not exceed 0.2 kcal/mol. Therefore, using the MP2/6-311G** frequencies (scaled by 0.94) in G2 calculations, decreases only slightly the differences between corresponding transition states and molecular complexes, and the energies of the transition states are still below the reactants and the respective molecular complexes.

Both MC1a and MC3 are weakly bound molecular complexes. A basis set superposition error (BSSE) for these structures can be estimated by the counterpoise corrections.[15] Calculation of the interaction energy of $CH_3OH + F$ system leads, at the MC1a structure, to the same value of 0.5 kcal/mol

Hydrogen Abstraction from Methanol. 1

J. Phys. Chem. A, Vol. 102, No. 46, 1998 **9223**

TABLE 2: Relative Energies of Stationary Points of the Potential Energy Surface at 0 K for the CH₃OH + F Reacting System, Calculated at Different Levels of Theory, with Respect to the Reactant Energy (the Reaction Enthalpies at 298 K Are in Bold Type)

molecular system	PMP2[a]	MP4[b]	G2MP2	G2MP3	G1	G2	exp[c]
CH₂OH + HF	−38.1	−33.5	−40.6	−39.5	−38.6	−40.1	
	−37.5	**−32.9**	**−40.0**	**−38.9**	**−38.0**	**−39.5**	**−39.9 ± 1.0**
FH···CH₂OH (MC2)	−44.6	−39.9	−45.5	−44.6	−44.0	−45.0	
F···H···CH₂OH (TS2)	0.6	0.8	−6.5	−6.4	−6.7	−6.8	
MC3	−2.0	−2.3	−3.5	−3.6	−3.4	−3.6	
TS3	−3.5	0.7	−5.1	−4.2	−4.3	−4.8	
CH₃OF···F (MC1a)	−1.2	−1.2	−0.7	−0.7	−0.5	−0.7	
CH₃O···H···F (TS1)	4.1	4.0	−2.5	−2.3	−2.9	−2.9	
CH₃O···HF (MC1b)	−33.8	−32.7	−36.5	−36.3	−35.4	−36.5	
CH₃O + HF	−27.1	−26.1	−31.2	−30.8	−30.2	−31.3	
	−26.7	**−25.7**	**−30.8**	**−30.4**	**−29.8**	**−30.9**	**−30.8 ± 1.0**

[a] PMP2/6-311G**//MP2/6-311G** energy with ZPE calculated on base of the nonscaled MP2/6-311G** frequencies. *[b]* MP4SDTQ/6-311G**// MP2/6-311G** energy with ZPE calculated on base of the nonscaled MP2/6-311G** frequencies. *[c]* Calculated on base of the enthalpies of formation from ref 13.
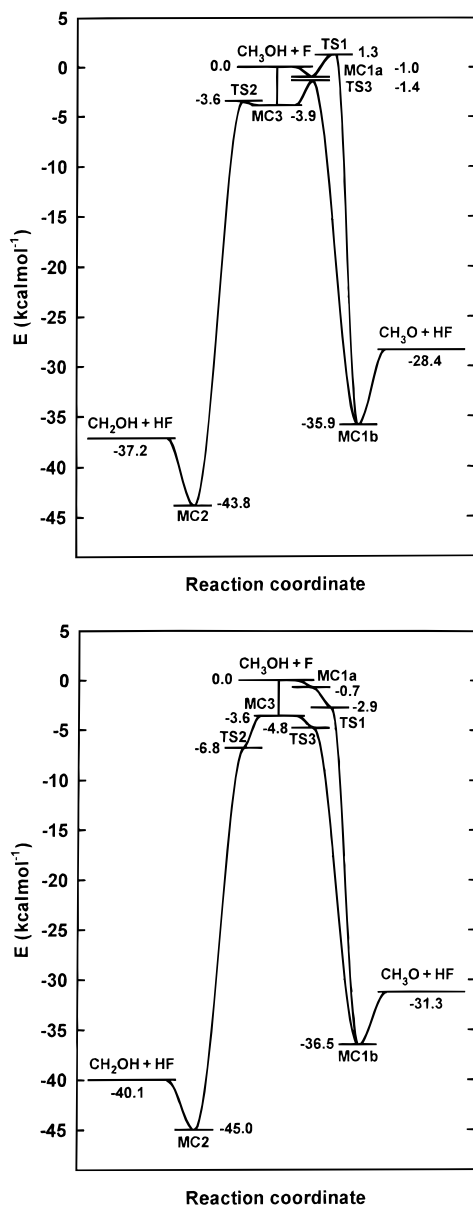

Figure 2. Schematic energy profile for CH₃OH + F reaction. The energies are calculated at the G2 level, (a) without zero-point energy corrections (ZPE), (b) taking into account ZPE corrections.

at MP2/6-31G*, MP2/6-311G**, and MP4SDTQ/6-311G**// MP2/6-311G** levels. The BSSE amounts to 1.6 kcal/mol (MP2/6-31G*) and 1.1 kcal/mol (MP2, MP4/6-311G**). For the molecular complex MC3 this error was found to be 2.9 kcal/mol (MP2/6-31G*) and 2.0 kcal/mol (MP2, MP4/6-311G**). Thus, taking into account the BSSE leads to a lowering of the stabilization energy in complexes MC1a and MC3. However, this is not important in the kinetic description of the reaction system as the major role is played by the energy barrier related to the second elementary step.

The shape of the potential energy profiles for the reaction channels are very sensitive to the level of calculation used. We believe that the most credible results are those obtained at the G2 level. This is confirmed by G2-values of the reaction enthalpy which were found very close to experiment for both reaction channels. It is important to note that all characteristic points of the potential energy surface are located below the reactant energy level at 0 K. Therefore, the molecular complexes must appear along the reaction path between reactants and respective transition states. The molecular complexes MC1a and MC3 are not stable energetically after inclusion of ZPE, which suggests that assuming no energy barrier for all the second elementary steps should be a realistic approach for further calculations of the rate constant. The elementary processes which lead from reactants to respective molecular complexes of the channel products proceed without any energy barrier. Therefore, unimolecular dissociation/recombination processes play an important role in the description of reaction kinetics. Analysis of the results of Glauser and Koszykowski[7] also leads to similar conclusions. Their calculated overall rate constant (R1 + R2), in the zero-energy barrier assumption, is about 5 times lower than experimental values. We think that this large disagreement is essentially related to the preexponential factor. This indicates that it is not possible to get higher values of the calculated rate constant using transition state theory. Thus, the reaction mechanism must be determined by unimolecular processes. This is confirmed by the very high value of the experimental rate constant[5] $(1.1-1.7) \times 10^{-10}$ cm³ molecule⁻¹ s⁻¹ which is close to the gas-kinetic frequency.

3. Rate Constant Calculation

3.1. Method Used. Formation of a stable intermediate may lead to a negative activation energy or strongly curved Arrhenius plots for apparently elementary gas-phase reactions. In the past several years, Mozurkevich and Benson[16] and Chen et al.[17] have developed theoretical models for the description of kinetics of a bimolecular reaction which proceeds via an intermediate complex. In the same spirit, and on the basis of RRKM theory, we have obtained a general expression for a reaction rate constant in the case of a bimolecular reaction in which two
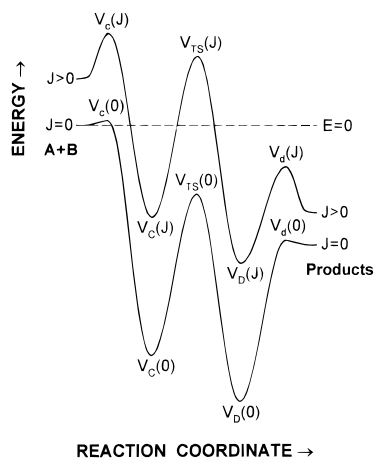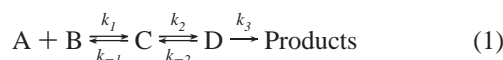
Figure 3. Schematic energy profile for a reaction A + B proceeding through two molecular complexes V_c and V_d separated by a transition state V_{TS}.

intermediate complexes are formed. The reaction is described according to the following reaction:

$$A + B \underset{k_{-1}}{\overset{k_1}{\rightleftharpoons}} C \underset{k_{-2}}{\overset{k_2}{\rightleftharpoons}} D \overset{k_3}{\rightarrow} \text{Products} \qquad (1)$$

where A and B are reactants having enough energy to form the final products, and C and D are intermediate complexes. A representative potential energy profile of that system is shown in Figure 3. Lower case c and d denote "activated complexes" used in the description of the kinetics of unimolecular dissociation/recombination processes, and TS denotes a transition state for the second elementary step. As shown in Figure 3, we assume that the elementary processes at the first and third elementary steps proceed without any energy barrier while the elementary reactions at the second elementary step are characterized by an energy barrier with respect to the molecular complexes C and D, corresponding to the transition state TS. The potential energy of the respective structures at 0 K is given by $V_i(0)$, where $i =$ c, TS, d. If the intermediates are rotating, the conservation of angular momentum J requires some minimum of rotational energy, $U_i(J)$, which is added to the potential energy to get an effective potential, $V_i(J)$

$$V_i(J) = V_i(0) + U_i(J) \qquad (2)$$

The potential energy denoted for abbreviation as V_i is always related to $V_i(0)$. As shown in Figure 3, the potential curve labeled $J > 0$ includes the rotational energy. Except for the activated complexes c and d, we also assume that the geometries of other structures do not depend on E and J.

The concentrations of species as well as the rate constants for elementary steps should be functions of the total energy E and angular momentum J. The reaction rate is given by

$$-\frac{d[A]}{dt} \equiv k_{obs}[A][B] = \frac{\int_{V_m}^{\infty} dE \sum_{J=0}^{J_m} k_3(E, J)[D(E, J)]f_D(E)}{\int_{V_D}^{\infty} f_D(E') dE'} \qquad (3)$$

where k_{obs} is the rate constant observed experimentally, V_m is the largest value of $V_i(0)$ and $J_m(E)$ is the maximum angular momentum for which reaction can take place with energy not higher than E. It is determined by the conditions

$$J_m(E) = \min\{J_c, J_{TS}, J_d\} \qquad (4)$$

where J_i ($i =$ c, TS, d) are the largest integers which satisfy the inequality

$$V_i(0) + U_i(J_i) \leq E \qquad (5)$$

while $f_D(E)$ denotes the weights of the Boltzmann distribution for states of intermediate D at energy E.

In order to obtain the expression of the experimentally observed rate constant k_{obs}, a Boltzmann distribution is assumed for the concentration of the states of the intermediates, $[C(E,J)]$ and $[D(e,J)]$. RRKM theory is then used to express the microcanonical rate constants, $k_i(E,J)$. Neglecting the feedback between C and D is equivalent to assuming that at any E and J, the intermediate complex C is formed mainly by bimolecular combination of A and B, so that

$$k_1(E,J)[A(E,J)][B(E,J)] \gg k_{-2}(E,J)[D(E,J)] \qquad (6)$$

This inequality should be fulfilled very well for the scheme described in Figure 3 for the following reasons: For fast and very fast reactions such as those studied here, the forward processes are dominant. In addition, the reverse reaction corresponding to the second elementary step is associated with an energy barrier, which is not the case for the first step corresponding to a barrier less association reaction.

Under steady-state conditions, one can, after some algebra, obtain a RRKM-like expression for the rate constant k_{obs}

$$k_{obs} = \frac{z}{hQ_AQ_B} \int_{V_m}^{\infty} dE \sum_{J=0}^{J_m}$$
$$W_c(E,J) \frac{W_{TS}(E,J)}{W_c(E,J) + W_{TS}(E,J)} \frac{W_d(E,J)}{W_d(E,J) + W_{TS}(E,J)}$$
$$\exp(-E/RT) \quad (7)$$

The center of mass motion partition function is assumed to have been factored out of the product of the partition functions of reactants Q_AQ_B, and is included in z. In general, in z can be also included the partition functions related to those inactive/adiabatic degrees of freedom which are not taken into account by the integral. $W_i(E,J)$ is the sum of states at energy lower than E and angular momentum J of the activated complex/transition state. The fractions under the sum correspond to the microscopic branching ratios at given E and J, for the second and third elementary steps of the investigated reaction in the forward direction. Therefore, the equation may be easily adapted to the form corresponding to the other reaction scheme. Equation 7 shows that all the computational effort is related to the calculation of the sum of states $W(E,J)$. This calculation depends on the level at which the angular momentum conservation is considered.

For reacting molecules with rotational constants $A_i \gg B_i \approx C_i$, the usual approximation of a two-dimensional (linear) rotor should work sufficiently well. The energy levels depend only on J, so that

$$U_i(J) = B_e J(J+1) \qquad (8)$$

with $B_e = 0.5(B_i + C_i)$. The remaining nonactive rotational degree of freedom, the rotation about the symmetry axis, is treated as one-dimensional rotor with a rotational constant, A_i. The sum of states $W_i(E,J)$ is then given by

$$W_i(E,J) = W_{vib,i}(E - U_i(J)) \, (2J + 1) \qquad (9)$$

where $W_{vib}(E_{vib})$, with $E_{vib} = E - U_i(J)$, denotes the sum of the vibrational states at the vibrational energy less than or equal to E_{vib}.

If all the rotational degrees of freedom of the activated complexes and transition states have to be considered, an approximation of prolate symmetry top rotors with rotational constants $A_i > B_i \approx C_i$, should lead to reasonable results. The rotational energy then depends on two quantum numbers J and K as follows:

$$U_i(J,K) = B_e J(J + 1) + (A_i - B_e) K^2 \qquad (10)$$

with K and the third quantum number M independently limited by J, i.e., $-J \leq K$, $M \leq J$. In this case the sum of states W_i-(E,J,K) is given by

$$W_i(E,J,K) = W_{vib,i}(E - U_i(J,K)) \, g_{JK} \qquad (11)$$

where g_{JK} is the degeneracy of the rotational level (J,K). Equation 7 for the "observed" rate constant is then replaced by

$$k_{obs} = \frac{z}{hQ_AQ_B} \int_{V_m}^{\infty} dE \sum_{J=0}^{J_m} \sum_{K=0}^{K_m} W_c(E, J, K)$$

$$\frac{W_{TS}(E, J, K)}{W_c(E, J, K) + W_{TS}(E, J, K)} \frac{W_d(E, J, K)}{W_d(E, J, K) + W_{TS}(E, J, K)}$$

$$\exp(-E/RT) \quad (12)$$

The sum over J at given energy E is limited by $J_m(E)$ according to eq 3, whereas the upper limit of $K_m(E,J)$ is determined by similar conditions

$$K_m(E, J) = \min\{K_c, K_{TS}, K_d\} \qquad (13a)$$

with

$$V_i(0) + U_i(J, K_i) \leq E \qquad \text{and} \qquad K_i \leq J \quad (13b)$$

The computational problem is then reduced to the calculation of the sums of vibrational states, $W_{vib}(E_{vib})$ which can be evaluated with a sufficient precision in terms of inverse Laplace transformation of a vibrational partition function using the steepest descent method.[18,19]

The sum of states of the transition state TS for the second elementary step can be straightforwardly calculated using eqs 10 and 11. These calculations are more elaborate in the case of the two transition states c and d (Figure 3) associated to barrierless processes. The geometries of c and d (often called "activated complexes") are indeed not well defined as they do not correspond to a true saddle point in the potential energy surface and their properties depend on E and J. A variational treatment is often used to find the location of the activated complex. In this type of theoretical approach,[20] the degrees of freedom are separated into conserved and transitional modes. This is particularly meaningful when the activated complexes are loose, i.e., when they are located at large separation of the reactants. For the description of unimolecular dissociation/recombination processes, several sophisticated methods exist such as the variational transition state theory[21] (VTST), the flexible transition state theory (FTST) and its new developments (Aubanel and Wardlaw,[22] Klippenstein and Marcus,[23] and Smith[24]) and the more recent work of Robertson, Wagner, and Wardlaw[25] on the canonical version of FTST (CFTST). These approaches require the computation of many ab initio electronic structure calculations to determine the angular potential over ranges of geometries along reaction paths. It is difficult to apply these methods in this complex reaction mechanism. For that reason, we have decided to use an alternative method, the statistical adiabatic channel model[26] (SACM) and specifically the simplified version (SSACM) developed by Troe and which was successfully used for the rate constant calculation of unimolecular reactions.[27,28] Its internal simplicity allows one to gain some insight into the molecular parameters of the structures involved in the reaction having the major contribution in the final value of the calculated rate constant. In the SACM approach, all the coordinates are decoupled in the activated complex, and are represented by harmonic-oscillator and rigid-rotor approximations. Coupling between the angular momenta of fragment rotations, fragment orbital motions, and overall angular momentum J is difficult to account for. For example, in the simplified version of SACM (SSACM), the individual reactant(s) and product(s) states are correlated without the angular momentum and symmetry constraints for any channel state, and the important couplings are introduced a posteriori by global coupling corrections.[27,28]

The general assumptions and simplifications made in this approach are as follows: (i) All vibrational coordinates of the dissociating molecule are separated into two classes: the *disappearing* oscillators which become product external rotors or orbital motions, and all the others considered as the *conserved* oscillators.

(ii) For a given angular momentum J, the lowest open channel is given by the centrifugal barrier, $E_o(J)$. The centrifugal barriers, $E_o(J)$ are derived from the maximums of the lowest channel potential, $V(q)$ as described in refs 27 and 28. It should be noted that Troe's SSACM predicts the occurrence of the threshold energy at $J = 0$ (for a loose activated complex this zero-point level is very small, below 1 cm^{-1} as shown in Figure 3.

(iii) The energy patterns of the channel maxima for the *disappearing* oscillators ϵ_i are derived from the transitional modes of the reactants and products by an interpolating function containing two empirical parameters: a looseness parameter α and a Morse parameter β. The interpolating function depends sensitively on the ratio α/β, but also on other energetic and structural parameters of the reactants and products (see for details refs 28 and 29). In the classical approach, a pseudopartition function of m disappearing oscillators Q_d is expressed as

$$Q_d = \prod_{i=1}^{m} \Gamma(1 + x_i)[1 - \exp(-\epsilon_i/RT)]^{-x_i} \qquad (14)$$

The exponents x_i corresponding to ϵ_i, which express (by a value between 0.5 and 1.0) a *rotational* or *vibrational* character of ϵ_i, are also derived by a similar interpolating procedure.

(iv) The energy pattern of the channel maxima for the conserved oscillators ϵ_j is expressed by a simple interpolation between the corresponding states of reactants and products as described in refs 28 and 29. The partition function Q_c for n modes of the conserved oscillators is calculated in the same way as in the case of "normal" oscillators, i.e.,

$$Q_c = \prod_{j=1}^{n}[1 - \exp(-\epsilon_j/RT)]^{-1} \qquad (15)$$

(v) Values of the model parameters α and β are derived as follows. The Morse parameter β is calculated in the usual way from the vibrational frequency ϵ_{RC}, which corresponds to the reaction coordinate

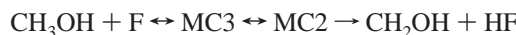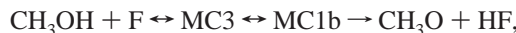$$\beta = \frac{\pi}{h}\epsilon_{RC}\sqrt{\frac{2\mu}{D}} \qquad (16)$$

where μ denotes the reduced mass of fragments. The looseness parameter α is often used as the fitting parameter to get a satisfactory agreement between values of calculated and experimental rate constants. For many unimolecular reactions studied, its "standard" value corresponds to the ratio of α/β close to 0.5. The "best" ratio of α/β was estimated to be 0.46 $\pm$ 0.09 in a comparative study of Cobos and Troe,[28] and we have used this recommended value in our calculation.

Other assumptions of the presented SSACM method are related to global coupling corrections and cannot be applied in our approach. According to assumptions i−v, the calculation of $W(E,J,K)$ requires the derivation of the centrifugal barriers $E_o(J)$ and, next, the estimation of the quanta for the disappearing and conserved oscillators, at given E and J.[28] One can expect that, for a loose activated complex, global coupling corrections are of minor importance. Then, the rotational energy is related to orbital motions of the activated complex, and for an assumed prolate symmetric top, with the rotational constants, A and B_{cent}-(J), is expressed by
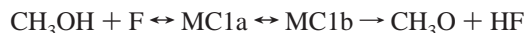
$$U(J,K) = E_o(J) - E_o(0) + (A - B_{cent}(J))\,K^2 \qquad (17)$$

According to eq 11, the determination of the sum of states $W(E,J,K)$ requires only the calculation of the sum of the vibrational states $W_{vib}(E - U(J,K))$. They can be evaluated by the inverse Laplace transformation of the product of the partition functions for the disappearing and conserved oscillators, $L^{-1}[Q_d(s)Q_c(s)/s]$, with $s = 1/RT$, using the steepest descent method.[19] The rate constant from eq 12 is then straightforwardly evaluated by exact numerical integration. If α and β are chosen as described in (v), then all the internal parameters of the SSACM method are related to each other or derived from the structural parameters obtained in ab initio calculations. Therefore, in this approach there are no fitting or adjustable parameters except for the choice of the level of the ab initio method used.

3.2. Results and Discussion. As shown in Figure 2b, inclusion of the zero-point vibrational energy at the G2 level causes the molecular complexes MC1a and MC3, which are located above energy levels of respective transition states, to be unstable energetically. This may be due to the fact that, in the G2 method, the energy, calculated at G2 level for a MP2 optimized geometry does not correspond exactly to the top of the saddle point. This leads to "negative" or zero energy barriers for the second elementary steps. Occurrence of similar "negative" energy barrier was also reported by Chen et al.[17] for the hydrogen abstraction from hydrocarbons by halogen atoms studied at G1 level. Calculation of rate constants for all reaction channels using eq 12 requires some additional model assumptions, related to the location of those "transition states". We assume that all transition states are located at the energy corresponding to the respective molecular complexes, i.e., TS2 and TS3 at energy level of MC3, and TS1 at energy level of MC1a. This is equivalent to the assumption of a zero energy barrier for the second elementary step of all investigated reaction channels, and should give a lowest limit of the calculated rate constants values. If we denote the rate constants corresponding to following reaction pathways:

$$CH_3OH + F \leftrightarrow MC3 \leftrightarrow MC1b \rightarrow CH_3O + HF,$$

$$CH_3OH + F \leftrightarrow MC3 \leftrightarrow MC2 \rightarrow CH_2OH + HF$$

and

$$CH_3OH + F \leftrightarrow MC1a \leftrightarrow MC1b \rightarrow CH_3O + HF$$

by k_{R1}, k_{R2}, and k'_{R1}, respectively, eq 12 for the rate constants under investigation should be rewritten as follows:

$$k_{R1} = \frac{z}{hQ_AQ_B}\int_0^\infty dE \sum_{J=0}^{J_m}\sum_{K=0}^{K_m}$$

$$W_{1a}(E, J, K)\frac{W_1^*(E, J, K)}{W_{1a}(E, J, K) + W_1^*(E, J, K)}$$

$$\frac{W_{1b}(E, J, K)}{W_{1b}(E, J, K) + W_1^*(E, J, K)}\exp(-E/RT) \quad (18a)$$

$$k_{R2} = \frac{z}{hQ_AQ_B}\int_0^\infty dE \sum_{J=0}^{J_m}\sum_{K=0}^{K_m}$$

$$W_3(E, J, K)\frac{W_2^*(E, J, K)}{W_3(E, J, K) + W_2^*(E, J, K) + W_3^*(E, J, K)}$$

$$\frac{W_2(E, J, K)}{W_2(E, J, K) + W_2^*(E, J, K)}\exp(-E/RT) \quad (18b)$$

$$k'_{R1} = \frac{z}{hQ_AQ_B}\int_0^\infty dE \sum_{J=0}^{J_m}\sum_{K=0}^{K_m}$$

$$W_3(E, J, K)\frac{W_3^*(E, J, K)}{W_3(E, J, K) + W_2^*(E, J, K) + W_3^*(E, J, K)}$$

$$\frac{W_{1b}(E, J, K)}{W_{1b}(E,k\,J, K) + W_3^*(E, J, K)}\exp(-E/RT) \quad (18c)$$

For brevity, the sum of states W and the threshold energies V, given in eqs 18a−c, are labeled by the index i corresponding to the respective transition state (denoted by *) or activated complex related to unimolecular dissociation of respective molecular complex TS_i or MC_i according to the notation used in Figure 3. The rate constant, k'_{R1} is related to an extra reaction pathway which leads, via MC3 and TS3, to the formation of methoxy radicals (see Figure 2). The other rate constants correspond to "real" reaction channels, R1 and R2. The rate constants, which lead to formation of hydroxymethyl, $k(CH_2OH)$ and methoxy, $k(CH_3O)$ radicals are given by $k(CH_2OH) = k_{R2}$ and $k(CH_3O) = k_{R1} + k'_{R1}$.

Description of unimolecular processes requires a choice of molecular parameters which describe an "activated complex". Separation of vibrational frequencies of intermediate complexes into two classes: the "disappearing" and "conserved" oscillators is quite clear. A comparison of vibrational frequencies of intermediate complexes with reactants and products modes shows that the frequencies higher than ν_4 (MC3, MC1a) and ν_6 (MC1, MC2) are, at any level of theory, almost unchanged compared to the isolated CH_3OH, CH_2OH, CH_3O, and HF species. The ν_3 frequency of all molecular complexes, corre-

Hydrogen Abstraction from Methanol. 1

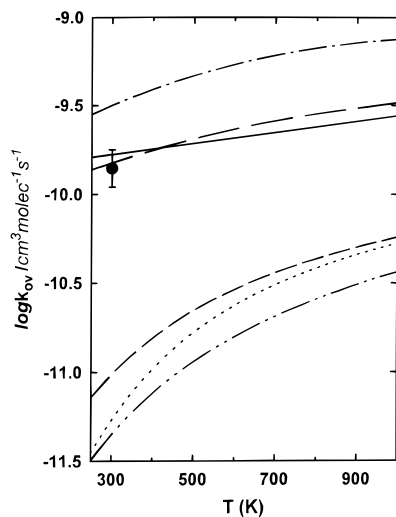*J. Phys. Chem. A, Vol. 102, No. 46, 1998* **9227**

Figure 4. The overall rate constants, k_{ov} measured experimentally[5] (circle) and calculated at different levels of theory (lines) from molecular parameters obtained by G2 method with scaled SCF/6-31G* frequencies ($\cdot$ −), G2 with scaled MP2/6-31G* frequencies (solid line), G2 with scaled MP2/6-311G** frequencies (long dashed line), PMP2/6-311G** with frequencies as above (short dashed line), MP4SDTQ/6-311G**// MP2/6-311G** with frequencies as above (dotted line), PMP2/6-31G* with scaled MP2/6-31G* frequencies ($\cdot\cdot$ −).

TABLE 3: Calculated Rate Constants for the Formation of CH₃O (k_{R1} and k'_{R1}) and CH₂OH (k_{R2}), and the Rate Constants for Formation of Molecular Complexes MC1a and MC3 (Definition of the Symbols in Text) in Units 10^{-11} cm³ molecule⁻¹ s⁻¹

T(K)	$k_{R1}{}^a$		k_{MC1a}	$k'R1{}^b$		$k_{R2}{}^c$		k_{MC3}
300	9.72	$(0.88)^d$	9.72	0.23	(0.21)	6.99	(6.20)	7.22
400	11.5	(0.97)	11.5	0.23	(0.19)	7.41	(6.28)	7.63
500	13.0	(1.09)	13.0	0.23	(0.19)	7.87	(6.44)	8.09
800	16.0	(1.50)	16.0	0.24	(0.19)	9.11	(7.09)	9.35
1000	17.2	(1.77)	17.2	0.26	(0.20)	9.88	(7.59)	10.1

^{a} Rate constant for reaction: CH₃OH + F → MC1a ⇌ MC1b → CH₃O + HF. ^{b} Rate constant for reaction: CH₃OH + F → MC3 ⇌ MC1b → CH₃O + HF. ^{c} Rate constant for reaction: CH₃OH + F → MC3 ⇌ MC2 → CH₂OH + HF. ^{d} In brackets the rate constant value when the back dissociation of MC1a or MC3 is considered.

sponding to the stretching mode of the respective breaking bond, was considered as the 'reaction coordinate' mode, and used for the estimation of the Morse parameters β according to eq 30. The corresponding α values were derived from the recommended[28] ratio of $\alpha/\beta = 0.46$, so that all parameters used in the calculation are described by the molecular data given in Tables 1a and b.

Results of the rate constant calculations are shown in Figure 4. A zero energy barrier was assumed for the transition states which have their total energy lower than the one of their respective molecular complexes. The overall rate constant, k_{ov} = k(CH₃O) + k(CH₂OH), calculated with the molecular parameters of the stationary points obtained at MP2/6-31G*, MP2/6-311G**, and MP4SDTQ/6-311G**//MP2/6-311G** levels, is significantly underestimated. At 300 K, the constant is more than 1 order of magnitude smaller than the experimental value. This result is a consequence of the nonzero energy barrier for the second elementary step and is also due to the back dissociation of MC3 and MC1a in the first elementary step. At the G2 level both molecular complexes, MC1a and MC3 are not stable and the overall rate constant k_{ov} for total formation of H-abstraction products should be equal to the sum of the rate constants for the unimolecular recombination giving MC1a (k_{MC1a}) and MC3 (k_{MC3}). The structures of molecular complexes MC1a and MC3 are only used for the determination of the molecular parameters necessary for the description of the unimolecular processes. Therefore, neglecting, in the second elementary step, the back dissociation of MC1a and MC3 (which corresponds to the neglect of $W_{1a}(E,J,K)$ and $W_3(E,J,K)$ in the denominators of the first fractions in eqs 18a−c) should lead to realistic values of calculated k_{R1}, k_{R2}, and k'_{R1}. In this way, k_{R1} and $k_{R2} + k'_{R1}$ are equal to the rate constants for formation of molecular complexes, MC1a (k_{MC1a} and MC3 (k_{MC3}), respectively (due to the strong exothermicity of reactions R1 and R2, contributions of the last fractions of the integrals (eqs 18a−c) are close to unity even at the highest temperature considered in this study).

The use of structural parameters obtained at the G2 level, i.e., (U)HF/6-31G* vibrational frequencies scaled by 0.8929 and

rotational constants of the MP2/6-31G* optimized geometries, leads to a significant overestimation of the calculated rate constants. At 300 K, the rate constants $k_a = 1.2 \times 10^{-10}$ cm³ molecule⁻¹ s⁻¹ and $k_b = 2.6 \times 10^{-10}$ cm³ molecule⁻¹ s⁻¹, are almost 3 times higher than the overall rate constant $k_{ov} = k_{MC1a}$ + k_{MC3} measured experimentally at room temperature. This may be explained as the result of incorrect vibrational frequencies of molecular complexes used in the calculation. The complexes are very loose, especially MC3, so that the lowest frequencies (transitional modes) may influence significantly the final results of the calculated rate constants. The smallest SCF frequencies are usually underestimated, and considerably less realistic than those obtained in the MP2 geometry optimization, e.g., the two lowest nonscaled frequencies of MC3 of 39 and 47 cm⁻¹ (SCF/6-31G*), and 44 and 51 cm⁻¹ (SCF/6-311G**) are almost 2 times lower than their MP2 counterparts of 83 and 132 cm⁻¹ (MP2/6-31G*), and 72 and 84 cm⁻¹ (MP2/6-311G**). The typical scaling factor for MP2 frequencies, which takes into account their overestimation compared to experimental values is 0.94, and this value was used in this study. Of course, to be in full agreement with the G2 methodology,[11] we should use individual scaling factors for each structure, which reproduces the ZPE correction obtained at (U)(HF/6-31G*, in order to maintain the same total energy at 0 K. However, in this case, where the molecular complexes MC3 and MC1a are not stable, and exist only virtually, the use of one global scaling factor does not introduce changes in the relative total energies, important enough to play a role in calculation of rate constants (total energy of "transition states" was assumed equal to the one of molecular complexes).

The use of scaled MP2 frequencies causes an increase of the Morse parameters β and leads to smaller unimolecular rate constants, especially in the case of k_{MC3}. There are no significant differences in the respective vibrational frequencies of the optimized structures obtained with the 6-31G* and 6-311G** basis sets. Therefore, the overall rate constants calculated using the MP2/6-31G* and MP2/6-311G** vibrational frequencies differ from each other only slightly and are close to the experimental value at room temperature. We prefer to use the MP2/6-31G* frequencies in order to be more in line with the G2 approach which takes the MP2/6-31G* optimized geometry as reference. The details of the rate constant calculations are given in Tables 3 and 4. For comparison, the values of k_{R1}, k_{R2}, and k'_{R1}, which take into account the back dissociation of MC3 and MC1a, are listed in brackets. As can be seen, the temperature dependence of the overall rate constant is weak, and the rate constant, k_{ov} increases by 60% when the temperature rises from 300 to 1000 K. The total rate constant for formation of methoxy radicals k(CH₃O) depends slightly

TABLE 4: Calculated Rate Constants for the Formation of CH_3O, $k(CH_3O)$, and CH_2OH, $k(CH_2OH)$, and the Overall Rate Constant k_{ov}, and the Branching Ratio of Methoxy Radicals $\Gamma(CH_3O)$

T (K)	$k(CH_3O)$ (cm^3 molecule^{-1} s^{-1})	$k(CH_2OH)$ (cm^3 molecule^{-1} s^{-1})	$k_{ov,calc}{}^a$ (cm^3 molecule^{-1} s^{-1})	$k_{ov,exp}$ (cm^3 molecule^{-1} s^{-1})	$\Gamma(CH_3O)^b$ calcd	exptl
300	9.95×10^{-11}	6.99×10^{-11}	1.69×10^{-10}	$(1.1-1.7) \times 10^{-10}$ ^{c}	0.59	0.57 ± 0.05^d
400	1.17×10^{-10}	7.41×10^{-11}	1.92×10^{-10}		0.61	
500	1.32×10^{-10}	7.87×10^{-11}	2.11×10^{-10}		0.63	0.62 ± 0.05^e
800	1.62×10^{-10}	9.11×10^{-11}	2.53×10^{-10}		0.64	
1000	1.74×10^{-10}	9.82×10^{-11}	2.73×10^{-10}		0.64	

^{a} $k_{ov} = k(CH_3O) + k(CH_2OH)$. ^{b} $\Gamma(CH_3O) = k(CH_3O)/k_{ov}$. ^{c} From ref 5. ^{d} From ref 5e at 298 K. ^{e} From ref 5e at 482 K.

more strongly on temperature than the rate constant for the formation of hydroxymethyl $k(CH_2OH)$. If the temperature changes from 300 to 1000 K, the rate constants, $k(CH_3O)$ and $k(CH_2OH)$ increase respectively by 75% and 40% compared to their value at 300 K. This explains the weak increase of the methoxy branching fraction with temperature, from 0.59 at 300 K to 0.64 at 1000 K. It is interesting to note that the contribution of k'_{R1} to $k(CH_3O)$ (the reaction proceeds via MC3 and TS3) is negligible. Whatever the temperature, about 97% of MC3 undergoes reaction leading to hydroxymethyl channel products. Therefore, if the back dissociation of MC3 is omitted, $k(CH_2OH)$ is almost equal to the unimolecular rate constant for the formation of MC3 k_{MC3}. The rate constant for formation of MC1a, k_{MC1a} is greater than k_{MC3} and also shows a larger increase with temperature. If we take into account the back dissociation of MC1a, this reaction is dominant due to the very small dissociation energy of MC1a (200 cm^{-1}). When this process is neglected, the rate constant for formation of MC1a is close to $k(CH_3O)$ as the efficiency for the formation of CH_3O by the reaction pathway related to k'_{R1} is considerably less important. Small values of k'_{R1} lead to the conclusion that the transition state TS3 does not play any important role in the kinetics of the $CH_3OH + F$ reaction system.

Calculated rate constants for the total formation of the channel products can be expressed in a convenient form for the use in chemical modeling studies

$$k(CH_3O) =$$
$$1.0 \times 10^{-10}(T/300)^{0.50} \; cm^3 \; molecule^{-1} \; s^{-1} \quad (19a)$$

$$k(CH_2OH) =$$
$$6.9 \times 10^{-11}(T/300)^{0.27} \; cm^3 \; molecule^{-1} \; s^{-1} \quad (19b)$$

The temperature dependence of both rate constants is weak as one can expect for unimolecular recombination. Results of the computed overall rate constant can be compared with experiments. Direct measurements[5] of k_{ov} at 300 K give an estimation of $(1.1-1.7) \times 10^{-10}$ cm^3 molecule^{-1} s^{-1}. Our results of $k(CH_3O) = 1.0 \times 10^{-10}$ cm^3 molecule^{-1} s^{-1} and $k(CH_2OH) = 7.0 \times 10^{-11}$ cm^3 molecule^{-1} s^{-1} lead to the overall rate constant $k_{ov} = 1.7 \times 10^{-10}$ cm^3 molecule^{-1} s^{-1} at 300 K. Agreement is then very good and the theoretical value corresponds to the upper limit of experimental results. On the other hand, the rate constants calculated for unimolecular processes are the limiting high-pressure values, so that they should be higher than those observed in the intermediate pressure range. There is no experimental information about possible influence of total pressure on measured rate constant values. However, according to the $CH_3OH + F$ reaction mechanism obtained in this study the rate constants for both reaction channels should be considered as the high-pressure limiting values.

Results of measurements of the branching ratios differ themselves considerably. However, a great part of recent measurements shows the methoxy branching fraction to be higher than 50%. Results of Durant[5e] of 0.6 ± 0.2 and Dóbé et al.[5f] of 0.57 ± 0.05 for the methoxy branching ratio at room temperature are in excellent agreement with our calculated value. The weak dependence on temperature is also in agreement with experimental estimations. It confirms that theoretical rate constants derived in this study describe well kinetics of the reaction studied.

Reverse Reactions $CH_3O + HF$ and $CH_2OH + HF$. The calculated potential energy surface also allows an evaluation of the rate constants for the reverse reactions: $CH_3O + HF \rightarrow CH_3OH + F (-R1)$ and $CH_2OH + HF \rightarrow CH_3OH + F (-R2)$ using the equilibrium constants obtained theoretically from molecular parameters of reactants and products. Obtained by this way, the rate constants, k_{-R1} and k_{-R2} can be expressed as

$$k_{-R1} =$$
$$1.5 \times 10^{-11}\exp(-15740/T) \; cm^3 \; molecule^{-1} \; s^{-1} \quad (20a)$$

$$k_{-R2} =$$
$$3.6 \times 10^{-12}\exp(-19860/T) \; cm^3 \; molecule^{-1} \; s^{-1} \quad (20b)$$

Both reactions ($-R1$) and ($-R2$) are strongly endothermic and very slow with rate constants at 300 K of 2.5×10^{-34} and 6.4×10^{-41} cm^3 molecule^{-1} s^{-1} for k_{-R2}, respectively. Therefore, the reverse reactions ($-R1$) and ($-R2$) do not play any role in subsequent rearrangements of methoxy and hydroxymethyl radicals.

4. Conclusion

Ab initio calculations at different levels of theory and using several basis sets were used to obtain structural parameters (optimized geometries, barrier heights, and vibrational frequencies) of the stationary points of the potential energy surface for the $CH_3OH + F$ reaction system. The reaction enthalpy values calculated at the G2 level are in very good agreement with those experimentally estimated. Results of calculations show that the mechanism of hydrogen abstraction from methanol by fluorine atoms is considerably more complex than was expected previously. This reaction proceeds with formation of intermediate complexes, and the energy profile for the $CH_3OH + F$ reaction system depends significantly on the level of theory used. At the most sophisticated level of theory, the G2 method, used in this work, all the characteristic points of the potential energy surface (transition states, molecular complexes) lie below reactant energy. This is certainly due to the fact that the G2 energy is not calculated for geometries optimized at this level, but at the MP2/6-31G(d) level. As the energy differences between the transition states and the corresponding molecular complexes are very small, they can be considered as not far from zero. The molecular complexes which precede the respective transition states are not stable energetically after inclusion of the zero-point vibrational energy and lead to apparent "negative" energy barriers. This implies that a zero

Hydrogen Abstraction from Methanol. 1

J. Phys. Chem. A, Vol. 102, No. 46, 1998 **9229**

energy barrier can be assumed for the second elementary steps and therefore, unimolecular processes will play an important role in the description of H-abstraction mechanism for CH_3OH + F reaction. It is also an explanation for the very high value of the overall rate constant, close to the gas-kinetic frequency, observed experimentally.

We propose a method for rate constant calculations of a bimolecular reaction which proceeds through formation of two loose intermediate complexes. General equations are derived on the basis of RRKM theory and adapted by us using the simplified version of the statistical adiabatic channel model developed by Troe.[28] In our approach, all the internal parameters necessary for the sum of states calculations, were determined using molecular properties, in particular, G2 energies and scaled MP2 vibrational frequencies, obtained from ab initio calculations, without any fitting or adjustable parameters.

Even if the barrierless steps of the reaction are treated in a simplified way, the calculated overall rate constant as well as the yield of the methoxy branching fraction correctly reproduce both qualitatively and quantitatively experimental ones. This study brings out the interesting nature of this reaction which is more complex than expected. Derived expressions for the site-specific rate constants, $k(CH_3O)$ and $k(CH_2OH)$ allow the description of the reaction kinetics over a wide range of temperatures. This has a significant importance for the chemical modeling studies, due to the lack of experimental rate constants measurements at higher than ambient temperature.

Supporting Information Available: Tables of optimized structures and vibrational frequencies of the potential energy surface (2 pages). Ordering information is given on any current masthead page.

References and Notes

(1) (a) Marshall, E. *Science* **1989**, *246*, 199. (b) Russel, A. G.; Pierre, D. S.; Milford, J. B. *Science* **1990**, *247*, 201.

(2) (a) Eyzat, P. *Rev. Assoc. Fr. Tech. Pet.* **1975**, *230*, 31. (b) Aronowitz, D.; Naegell, D. W.; Glassman, I. *J. Phys. Chem.* **1977**, *81*, 2555. (c) Westbrook, C. K.; Dryer, F. L. *Combust. Flame* **1980**, *37*, 171. (d) Spindler, K.; Wagner, H. Gg. *Ber. Bunsen-Ges. Phys. Chem.* **1983**, *86*, 2. (e) Norton, T. S.; Dryer, F. L. *Int. J. Chem. Kinet.* **1990**, *22*, 219.

(3) Bogan, D. J.; Setser, D. W. *ACS Symp. Ser.* **1978**, *66*, 237.

(4) (a) MacDonald, R. G.; Sloan, J. J.; Wassell, P. T. *Chem. Phys.* **1979**, *41*, 201. (b) Dill, B.; Heydtmann, H. *Chem. Phys.* **1980**, *54*, 9. (c) Hoyermann, K.; Lotfield, N. S.; Sievert, R.; Wagner, H. Gg. *18th International Symposium on Combustion.* (d) Meier, V.; Grotheer, H. H.; Just, T. *Chem. Phys. Lett.* **1984**, *106*, 97. (e) Wickramaaratchi, M. A.; Setset, D. W.; Hildebrandt, H.; Korbitzer, B.; Heydtmann, H. *Chem. Phys.* **1985**, *94*, 109. (f) Agrawalla, B. S.; Setser, D. W. *J. Phys. Chem.* **1986**, *90*, 2450.

(5) (a) Khatoon, T.; Hoyermann, K. *Ber. Bunsen-Ges. Phys. Chem.* **1988**, *92*, 669. (b) Pagsberg, P.; Munk, J.; Sillesen, A.; Anastasi, C. *Chem. Phys. Lett.* **1988**, *146*, 375. (c) McCaulley, J. A.; Kelly, N.; Golde, M. F.; Kaufman, F. *J. Phys. Chem.* **1989** *93*, 1014. (d) Bogan, D. J.; Kaufman, M.; Hand, C. W.; Sanders, W. A.; Brauer, B. E. *J. Phys. Chem.* **1990**, *94*, 8128. (e) Durant, J. L., Jr. *J. Phys. Chem.* **1991**, *95*, 10701. (f) Dóbé, S.; Bérces, T.; Temps, F.; Wagner, H. Gg.; Ziemer, H. In *Proceedings of the 25th International Symposium on Combustion*; Combustion Institute: Pittsburgh, 1994; p 775.

(6) Tsang, W. *J. Phys. Chem. Ref. Data* **1987**, *16*, 471.

(7) Glauser, W. A.; Koszykowski, M. L. *J. Phys. Chem.* **1991**, *95*, 10705.

(8) Frisch, M. J.; Trucks, G. W.; Schlegel, H. B.; Gill, P. M. W.; Johnson, B. G.; Wong, M. W.; Foresman, J. B.; Robb, M. A.; Head-Gordon, M.; Replogle, E. S.; Gomperts, R.; Andres, J. L.; Raghavachari, K.; Binkley, J. S.; Gonzalez, C.; Martin, R. L.; Fox, D. J.; Defrees, D. J.; Baker, J.; Stewart, J. P.; Pople, J. A., Eds.; Gaussian Inc.: Pittsburgh, PA, 1993. *Gaussian 94*, Revision D.3; Frisch, M. J.; Trucks, G. W.; Schlegel, H. B.; Gill, P. M. W.; Johnson, B. G.; Robb, M. A.; Cheeseman, J. R.; Keith, T.; Petersson, G. A.; Montgomery, J. A.; Al-Laham, M. A.; Zakrzewski, V. G.; Ortiz, J. V.; Foresman, J. B.; Cioslowski, J.; Stefanov, B. B.; Nanayakkara, A.; Challacombe, M.; Peng, C. Y.; Ayala, P. Y.; Chen, W.; Wong, M. W.; Andres, J. L.; Replogle, E. S.; Gomperts, R.; Martin, R. L.; Fox, D. J.; Binkley, J. S.; Defrees, D. J.; Baker, J.; Stewart, J. P.; Head-Gordon, M.; Gonzalez, C.; Pople, J. A., Eds. *Gaussian 92/DFT,* Revision F.2; Gaussian, Inc.: Pittsburgh, PA, 1995.

(9) Hehre, W. J.; Radom, L.; Schleyer, P.v.R.; Pople, J. A. *Ab Initio Molecular Orbital Theory*, Wiley: New York, 1986.

(10) Møller, C.; Plesset, M. S. *Phys. Rev.* **1934**, *46*, 618.

(11) (a) Pople, J. A.; Head-Gordon, M.; Raghavachari, K.; Curtiss, L. A. *J. Chem. Phys.* **1989**, *90*, 5622. (b) Curtiss, L. A.; Jones, C.; Trucks, G. W.; Raghavachari, K.; Pople, J. A. *J. Chem. Phys.* **1990**, *93*, 2537. (c) Curtiss, L. A.; Raghavachari, K.; Trucks, G. W.; Pople, J. A. *J. Chem. Phys.* **1991**, *94*, 7221. (d) Curtiss, L. A.; Raghavachari, K.; Pople, J. A. *J. Chem. Phys.* **1993**, *98*, 1293.

(12) Schlegel, H. B.; Sosa, C. *Chem. Phys. Lett.* **1988**, *145*, 329.

(13) (a) DeMore, W. B.; Sander, S. P.; Golden, D. M.; Hampson, R. F.; Kurylo, M. J.; Howard, C. J.; Ravishankara, A. R.; Kolb, C. E.; Molina, M. J. Chemical Kinetics and Photochemical Data for Use in Stratospheric Modeling. Evaluation No. 11; JPL Publ. 94-26; NASA Panel for Data Evaluation, Jet Propulsion Laboratory, California Institute of Technology: Pasadena, 1994; p 194. (b) Dóbé, S.; Bérces, T.; Turányi, T.; Márta, F.; Grussdorf, J.; Temps, F.; Wagner, H. Gg. *J. Phys. Chem.* **1996**, *100*, 19864.

(14) Stevens, P. S.; Brune, W. H.; Anderson, J. G. *J. Phys. Chem.* **1989**, *93*, 4068.

(15) van Duijneveldt, F. B.; van Duijneveldt-van de Rijdt, J. G. C. M.; van Lenthe, J. H. *Chem. Rev.* **1994**, *94*, 1873.

(16) Mozurkevich, M.; Benson, S. W. *J. Phys. Chem.* **1984**, *88*, 6429.

(17) (a) Chen, Y.; Tschuikow-Roux, E.; Rauk, A. *J. Phys. Chem.* **1991**, *95*, 9832. (b) Chen, Y.; Rauk, A.; Tschuikow-Roux, E. *J. Phys. Chem.* **1991**, *95*, 9900. (c) Chen, Y.; Tschuikow-Roux, E. *J. Phys. Chem.* **1993**, *97*, 3742.

(18) Robinson, P. J.; Holbrook, K. A. *Unimolecular Reactions*; Wiley: New York, 1972.

(19) (a) Forst, W.; Prášil, Z. *J. Chem. Phys.* **1969**, *51*, 3006. (b) Hoare, M. R. *J. Chem. Phys.* **1970**, *52*, 5695.

(20) Truhlar, D. G.; Garrett, B. C.; Klippenstein, S. J. *J. Phys. Chem.* **1996**, *100*, 12771.

(21) (a) Hase, W. L.; Wardlaw, D. M. In *Bimolecular Collisions*; Baggott, J. E., Ashford, M. N. R., Eds.; Burlington House: London, 1989; p 171. (b) Aubanel, E. E.; Wardlaw, D. M.; Zhu, L.; Hase, W. L. *Int. Rev. Phys. Chem.* **1991**, *10*, 249.

(22) Aubanel, E. E.; Wardlaw, D. M. *J. Phys. Chem.* **1989**, *93*, 3117.

(23) Klippenstein, S. J.; Marcus, R. A. *J. Chem. Phys.* **1987**, *87*, 3410; *J. Phys. Chem.* **1988**, *92*, 3105.

(24) Smith, S. C. *J. Chem. Phys.* **1991**, *95*, 3404; *J. Phys. Chem. 1993*, *97*, 7034.

(25) Robertson, S. H.; Wagner, A. F.; Wardlaw, D. M. *J. Chem. Phys.* **1995**, *103*, 2917.

(26) Troe, J. *J. Chem. Phys.* **1981**, *75*, 226.

(27) Troe, J. *J. Chem. Phys.* **1983**, *79*, 6017.

(28) Cobos, C. J.; Troe, J. *J. Chem. Phys.* **1985**, *83*, 1010.